

Elsevier required licence: © 2018. This manuscript version is made available under the CC-BY-NC-ND 4.0 license
<http://creativecommons.org/licenses/by-nc-nd/4.0/>

Evaluation of a new sponge addition-microbial fuel cell system for removing nutrient from low C/N ratio wastewater

Lijuan Deng^{a,b}, Huu-Hao Ngo^{c,*}, Wenshan Guo^c, Jie Wang^{a,b}, Hongwei Zhang^{a,b,*}

^a State Key Laboratory of Separation Membranes and Membrane Process, Tianjin Polytechnic University, Tianjin 300387, China

^b School of Environmental and Chemical Engineering, Tianjin Polytechnic University, Tianjin 300387, China

^c Centre for Technology in Water and Wastewater, School of Civil and Environmental Engineering, University of Technology Sydney, Sydney, NSW 2007, Australia

*Corresponding author, Email: hwzhang@tju.edu.cn; Tel: +86-13502171853

Email: haon@eng.uts.edu.au; Tel: +61-295142745

Abstract

This study developed a new microbial fuel cell (MFC) system (Sponge-MFC), which consisted of a cathodic chamber with an added sponge and two anodic chambers, for low carbon/nitrogen (C/N) wastewater treatment. When operating in the closed-circuit state, the Sponge-MFC(C) demonstrated its superior electrochemical performance compared to the closed-circuit MFC. This superiority took the form of higher coulombic efficiencies, voltage outputs, current densities and power densities. Adding a sponge could reduce the cathode's charge transfer resistance and solution resistance, and improve its capacitance, thus increasing cathodic reaction rate and power outputs. Simultaneous nitrification denitrification (SND) and bioelectrochemical denitrification processes on the cathode coupled with the sponge's SND process were responsible for efficient removal of nitrogen from the Sponge-MFC(C). Fluorescent in situ hybridization (FISH) analysis revealed that nitrifying bacteria and highly diversified denitrifying bacteria were distributed at the cathode's outer layer and inner layer, respectively. Higher phosphorus removal efficiencies ($82.06 \pm 1.21\%$) in the Sponge-MFC(C) than that in the MFC(C) ($53.97 \pm 2.32\%$) could be ascribed to biological phosphorus removal and precipitation of phosphate salts on the cathode. These results suggested the Sponge-MFC(C) could accomplish better

electrochemical behaviors and nutrient removal due to sponge addition when treating wastewater with low C/N ratio.

Keywords: Microbial fuel cell (MFC); Sponge; Low C/N; Bioelectrochemical denitrification; Denitrifying bacteria; Struvite precipitation

1. Introduction

Municipal and domestic wastewater generally has a low carbon to nitrogen (C/N) ratio, which is unfavorable for nitrogen and phosphorus removal during wastewater treatment when employing a biological nutrient removal (BNR) process [1]. Although it could be solved by adding external carbon sources, the overall treatment expense increased because of extra purchase cost, and the systems' intricate management and operation [2,3]. To date, much more effort has been devoted to the development of new processes for reducing carbon sources and aeration required for nutrient removal. These include, for example: a novel two-sludge system of anaerobic/anoxic/oxic (A^2/O) and biological contact oxidation [4]; a novel integrated system combining anaerobic ammonium oxidization and partial denitrification process [5]; an integrated partial nitrification, sludge fermentation, denitrification process in a sequencing batch reactor (PNSFD-SBR) [2]; and an upflow microaerobic sludge reactor (UMSR) [6]. However, these systems have suffered from complicated design, set-up, management and operation, and strict operational conditions (e.g. temperature).

Microbial fuel cell (MFC) is now considered to be a promising technology for integrated removal of carbon and nitrogen and generating energy. Viridis et al. [7] demonstrated the performance of a MFC-based system for combined carbon and nitrogen removal from wastewater. In their experiment, effluent from the anodic chamber went through an aerobic nitrification stage, which subsequently fed the cathodic chamber. Effective nitrogen removal could be realized at low C/N ratio (2.65-3.01 gCOD/g N) by NO_2-N or NO_3-N reduction on the cathode using electrons generated from the oxidation

of organic carbons at the anode. A later study conducted by Virdis et al. [8] assembled a MFC consisting of two compartments, in which the effluent from the anode chamber flew into the cathodic chamber, removing $76.8 \pm 0.5\%$ even at low C/N ratio of 1.88 ± 0.01 . This system accomplished both simultaneous nitrification and denitrification (SND) and bioelectrochemical denitrification at the cathode. A tubular dual-cathode MFC realized nitrification at the outer cathode and bioelectrochemical denitrification at the inner cathode, reaching high organic removal of 85-99% and total nitrogen (TN) removal of 66.7-89.6% and reducing the need for external organic compounds [9]. Zhang et al. [10] developed a single MFC with bottom anode and top rotating cathode under a continuous regime with a feeding C/N ratio of 5, which reduced nitrogen (TN removal of $91.5 \pm 7.2\%$) mainly through the cathodic autotrophic denitrification. Some studies also investigated the performance of MFC for phosphorus recovery and removal. Tao et al. [11] suggested that a two-chamber MFC could realize a great deal of total phosphorus (TP) removal mainly via chemical precipitation ($> 80\%$), but the high pH of the catholyte would seriously inhibit denitrification reaction. The increased addition of ammonium (NH_4) and magnesium (Mg) in MFC or magnesium ammonium phosphate (MAP) coupled with MFC in series also favored phosphorus precipitation [12,13]. Nevertheless, two main problems remain during the application of MFC systems in phosphorus removal: (1) the requirement of a high-pH zone through adding sodium hydroxide increased chemical cost; (2) the precipitated phosphorus deteriorated the cathode performance through limiting mass transfer of ions and oxygen. Moreover, there were only very few studies that have concentrated on phosphorus recovery and removal when treating wastewater with a low C/N ratio.

Currently, moving bed biofilm reactor (MBBR) has been developed as an improvement on the BNR process for treating various wastewaters [14]. The effectiveness of MBBR for low C/N wastewater treatment has been demonstrated in recent studies. Almomani et al. [15] operated a MBBR system (K3 AnoxKaldnes carriers) as post-treatment units for wastewater (WW) treatment lagoons for

six months. This system achieved significant $\text{NH}_4\text{-N}$ removal rates of 0.26 and 0.11 $\text{kg N/m}^3\cdot\text{d}$ at 20 °C and 1 °C, respectively. Additionally, various temperatures and the changes of WW sources ($\text{C/N} < 4$) did not influence the mass of attached biofilm on the carriers and did not inhibit the nitrifiers. Another study which investigated a nitrification/anammox process in a MBBR (Kaldnes biofilm carriers, filling ratio of 40%) found that Anammox bacteria outcompeting heterotrophic denitrifying bacteria utilized organic materials and reduced $\text{NO}_3\text{-N}$ in their role as electron acceptors under intermittent aeration mode for low C/N (< 0.5) wastewater treatment. Thus $\text{NO}_3\text{-N}$ concentration in effluent was smaller than the expected calculated values [16]. Chu and Wang et al. [17] employed biodegradable polymers polycaprolactone (PCL) (filling ratio of 11.3%) as the carbon source and attached growth media in a MBBR to treat low C/N (~ 0.7) wastewater, which realized high TN removal efficiency of 74.6% through the SND process at hydraulic retention time (HRT) of 18.5 h. Polyurethane (PU) sponge as an attached growth media has attracted much more attention in recent years and successfully removed nitrogen from wastewater via MBBR systems [18-20]. A new sponge that modified plastic carriers developed by Deng et al. [21] used in MBBR exhibited considerably higher nitrogen and phosphorus removal efficiencies than the MBBR with plastic carriers at short HRT of 6 h when treating synthetic domestic wastewater.

In this study, a novel system integrating a MFC with a MBBR was designed to improve treatment performance of MFC during low C/N wastewater treatment. To the best of our knowledge, this is the first study employing an MBBR with sponge as the cathodic chamber of an MFC (denoted as Sponge-MFC). The bioelectrochemical performance was explored in the Sponge-MFC and MFC (without sponge in the cathodic chamber) by conducting bioelectrochemical analyses (e.g. cyclic voltammetry (CV), electrochemical impedance spectroscopy (EIS), and linear sweep voltammetry (LSV)). Treatment performance was investigated in both of the Sponge-MFC and MFC through determining organic, nitrogen and phosphorus removals under closed- and open-circuit modes. Identification of

bacteria community and characterization of precipitates on the cathode were undertaken to assess the nutrient removal mechanism in the novel Sponge-MFC system.

2. Materials

2.1. Wastewater

A synthetic wastewater sample was prepared by dissolving glucose, ammonium sulfate, potassium dihydrogen orthophosphate and some trace nutrients in tap water to simulate low C/N ratio wastewater (C/N, 2.62 ± 0.12 in this study). The obtained synthetic wastewater contained 190-210 mg/L of chemical oxygen demand (COD), 60-75 mg/L of ammonium nitrogen ($\text{NH}_4\text{-N}$), and 6.6-7.0 mg/L of orthophosphate ($\text{PO}_4\text{-P}$). Sodium bicarbonate or sulfuric acid was added to adjust pH.

2.2. Microbial fuel cell construction and operation

Two identical loop-operated MFCs, designated MFC and Sponge-MFC (sponge added to the cathodic chamber), were constructed in this study (Fig. 1). Each MFC consisted of two anodic chambers with a working volume of 1 L per chamber and a middle cathodic chamber having a cathodic liquid volume of 3 L (Total reactor volume, TRV). The anodic and cathodic chambers were separated by Proton exchange membrane (PEM) (Nafion 117, Dupont, $15\text{ cm} \times 20\text{ cm}$). The anode was made of carbon felt with dimensions of $15\text{ cm} \times 15\text{ cm} \times 2\text{ cm}$. A cylindrical carbon felt (diameter 3 cm, length 15 cm) served as the cathode. The anodic chamber employed anaerobic sludge as the inoculum. The aerobic activated sludge taken from a local wastewater treatment plant was used to inoculate the cathodic chamber. The reticulated sponge cubes in the cathodic chamber of the Sponge-MFC were made of polyester polyurethane with density of $26\text{-}30\text{ kg/m}^3$, cell count of 80 cells/in (80 cells per 25.4 mm) and dimensions of 10 mm, 10 mm and 10 mm in length, width and thickness, respectively. The volume fraction of the cathodic chamber of 2% was filled with sponge cubes (60 sponge cubes in the

cathodic chamber). The anode and the cathode were connected externally using titanium wire by an external resistor with variable resistances. Ag/AgCl electrode was used as the reference electrode during the whole study period. The anodic chambers were fed by synthetic wastewater using two peristaltic pumps. The effluent from the anodic chambers directly went into the middle cathodic chamber. An air pump was employed to supply air to the cathodic chamber and dissolved oxygen (DO) concentration was controlled at 4.0-5.0 mg/L by an air flow meter. All of the MFC systems were operated under the intermittent mode (45 min “on” and 15 min “off”).

Fig. 1.

The whole study period was divided into five phases, namely Phase I (Day 0-15), Phase II (Day 16-30), Phase III (Day 31-45), Phase IV (Day 46-60) and Phase V (Day 61-90). Hydraulic retention times (HRTs) were controlled for the cathodic chamber at 12 h and 4 h for the anodic chamber accordingly. To acclimatize the biomass in the anodic and cathodic chambers, the closed-circuit Sponge-MFC and MFC (denoted as Sponge-MFC(C) and MFC(C), respectively) at Phases I, II and III were operated at external resistances of 1000, 100 and 50 Ω , respectively. Phase IV is the stabilization period for the Sponge-MFC(C) and the MFC(C) when operating at 50 Ω . The MFCs' performance in this study was evaluated under 50 Ω (Phase V). The initial sludge concentrations for each anodic and cathodic chamber were 5.0 and 3.0 g/L, respectively. The Sponge-MFC and MFC were operated under open-circuit (Sponge-MFC(O) and MFC(O), respectively) and closed-circuit conditions in parallel to evaluate the contribution of biological reaction and other removal processes (e.g. bioelectrochemical reaction, struvite precipitation) to the removal of nitrogen and phosphorus.

2.3. Analysis methods

The voltage (U) was recorded by a data acquisition unit (Agilent 34970A, Agilent Co., USA) every 15 minutes. The current (I) and the cell power output (P) were obtained according to Eqs. (1) and (2):

$$I = U/R \quad (1)$$

$$P = IU = U^2/R \quad (2)$$

where R is external resistance. Current density and power density were obtained by normalizing current and power output to the projected surface area of the anode, respectively.

Coulombic efficiency (CE) could be obtained from Eq. (3) [22]:

$$CE = \frac{M_s}{4F} \cdot \frac{I}{v_{An} \Delta c} \quad (3)$$

where M_s is the molecular weight of the substrate (glucose, 180.16 g/mol), F is the Faraday's constant (96,485 C/mol of electrons), b_{es} is the number of electrons exchanged per mole of oxygen (16 for glucose), v_{An} is the liquid volume of the anodic chamber, and Δc is the COD concentration difference.

COD, NH_4 -N, nitrite (NO_2 -N) and nitrate (NO_3 -N) concentrations were determined with Standard Methods (APHA, AWWA, WEF, 1998) using HACH DR/6000 colorimeter (HACH Co., USA). The Standard Methods were also employed for measurement of mixed liquor suspended solids (MLSS) concentration (APHA, AWWA, WEF, 1998).

Cyclic voltammetry (CV) was used to characterize the bioelectrochemical reaction of bacteria on the cathode in the Sponge-MFC(C) and MFC(C). A conventional three-electrode system was filled with 50 mM phosphorus buffer solution as an electrolyte and a medium containing NO_3 -N, whilst using the cathode as the working electrode, a platinum wire as the counter electrode, and an Ag/AgCl electrode as the reference electrode [23]. CV analyses were carried out in the system in the 0 to 600 mV range at a scan rate of 2 mV/s by employing a potentiostat/galvanostat (VersaSTAT 3, Princeton Applied Research). Electrochemical impedance spectroscopy (EIS) measurements were employed to record the impedance spectrum of the cathodes, which was conducted in a three-electrode mode in the

frequency range of 100 kHz to 1 MHz with an AC signal of 10 mV amplitude at open-circuit potential. Polarization and power density curves were obtained by linear sweep voltammetry (LSV), which was conducted three times at the scan rate of 1 mV/s over a range of 0.6 V using a potentiostat.

Scanning electron microscopy (SEM) analyses were done to characterize the morphology of biofilm on the cathode. When the experiment was completed, the preparation of biomass samples was subjected to the methods described by Xie et al. [24]. The dried precipitates were collected from the cathode using a plastic pipette tip [25]. The above samples were dried in a freeze drier, which were then coated with gold and subjected to SEM (Hitachi S4800, Japan). The dried precipitates from the cathode were also characterized by X-ray diffraction (XRD) (D8 ADVANCE, BRUKER) within the 10° to 70° range. Clear solutions for elemental analyses of the dried precipitates on the cathode were obtained according to the protocol proposed by Hao et al. [26]. The precipitates (40 mg) were dissolved in hydrochloric acid solution and subsequently into 250 mL of ultrapure water. The supernatant solution was filtered through a 0.45 µm membrane filter. The determination of Mg^{2+} , NH_4^+ and PO_4^{3-} in the clear solution was conducted by Ion Chromatograph (Dionex ICS-1100 and Dionex ICS-900, Thermo Scientific Dionex, USA, respectively).

2.4. *Fluorescent in situ hybridization (FISH)*

The collection of biofilm samples at the inner and outer layers of the carbon felt were carried out at the end of the experiment for both MFCs at closed- and open-circuit modes as described by Zhang et al. [27]. The biofilm derived from the cathode's surface was obtained by a sterilized razor, while a vortex shaker and a centrifuge served to obtain the inner biofilm samples. The fixation, hybridization and washing procedures for the biofilm samples were conducted as described by Amanm [28]. Oligonucleotides probes used in FISH experiments and their targeted microbial groups were selected according to preliminary results and listed in Table S1 in Supplementary Information. A Leica TCS

SP8 confocal laser-scanning microscope (CLSM) (Leica, Germany) with a 20X objective captured the images of all the samples. The images were further imported to ImageJ software for quantification [29].

3. Results and discussion

3.1. Performance of the Sponge-MFC(C) and MFC(C) during the start-up period

For the Sponge-MFC(C), the voltage output during Phase I (external resistance of 1000 Ω) experienced a linear-like increase from 62.01 mV, which reached a maximum value of 335.62 mV until Day 5, followed by a slight fluctuation within 10 days and finally stabilized at 309.04 mV on Day 15. When the external resistance decreased to 100 Ω on Day 16, a notable reduction trend in the voltage output was observed, ranging from 92.16 to 129.65 mV (Phase II). The voltage further declined to a lower range of 89.26-103.69 mV after a slight drop at 50 Ω during Phase III. The average cathodic potentials decreased from 199.49 ± 86.87 mV at 1000 Ω to 85.08 ± 31.32 mV at 100 Ω and 77.21 ± 17.08 mV at 50 Ω , respectively. The power densities increased when stepping down the external resistances, corresponding to 29.66 ± 3.18 mW/m² (1000 Ω), 41.74 ± 8.14 mW/m² (100 Ω) and 59.96 ± 5.24 mW/m² (50 Ω). The MFC(C) exhibited a similar change in voltage outputs as the Sponge-MFC(C), within the ranges of 156.73-221.59 mV, 73.75-87.77 mV and 66.75-81.11 mV during Phases I, II and III, respectively. As compared to the Sponge-MFC(C), lower cathodic potentials and power densities were obtained in the MFC(C) (130.19 ± 35.91 mV and 5.82 ± 1.35 W/m² at 1000 Ω , 67.02 ± 13.27 mV and 10.88 ± 1.03 W/m² at 100 Ω , and 63.86 ± 5.53 mV and 17.46 ± 1.14 W/m² at 50 Ω , respectively) in comparison to those for the Sponge-MFC(C). The unstable voltage outputs were ascribed to biofilm growth in both MFCs during the acclimatization period.

When both MFC systems reached steady status (50 Ω), the voltages of the Sponge-MFC(C) and the MFC(C) stabilized at 98.87 ± 5.16 mV and 72.89 ± 7.64 mV, resulting in current densities of 0.34 ± 0.08 A/m² and 0.23 ± 0.01 A/m² (power densities, 32.74 ± 1.68 and 16.06 ± 1.53 W/m²), respectively. The cathodic potential was maintained at higher values of 76.37 ± 1.23 mV vs SHE in the Sponge-

MFC(C) than in the MFC(C) (60.15 ± 1.47 mV vs SHE). These results indicated that enrichment and stabilization of nitrate- or nitrite-reducing bacteria were obtained on the cathode in both MFC systems. COD, $\text{NH}_4\text{-N}$, T-N and $\text{PO}_4\text{-P}$ removals in the Sponge-MFC(C) were $95.50 \pm 1.15\%$, $95.07 \pm 1.79\%$, $94.88 \pm 1.83\%$ and $83.85 \pm 1.80\%$, respectively, while the MFC presented poorer removal efficiencies ($93.04 \pm 1.16\%$, $79.35 \pm 3.62\%$, $75.49 \pm 3.73\%$ and $53.24 \pm 0.84\%$, respectively). Coulombic efficiencies (CEs) of the Sponge-MFC(C) and the MFC(C) were low at $22.62 \pm 4.80\%$ and $19.59 \pm 1.11\%$, respectively. The suspended-growth biomass in both MFC systems' cathodic chambers also reached steady state. Lower suspended sludge concentrations were found in the cathodic chamber of the Sponge-MFC(C) (4.1462 ± 0.1386 g/L) than in the MFC(C) (4.2683 ± 0.2512 g/L). This was explained as being due to the balance in the microorganism growth among suspended activated sludge and on and inside the sponge [30].

3.2. COD removal, voltage output and power generation of the Sponge-MFC(C) and MFC(C) during the operational period

During the operational period (Phase V), the major fraction of influent COD was removed by the anodic chamber for the Sponge-MFC(C) and MFC(C), with COD concentrations in the anode effluent of 10.59 ± 0.37 and 14.50 ± 1.64 mg/L, respectively. COD was further oxidized by the cathodic process as an aerobic polishing stage, which stabilized at 8.03 ± 0.78 and 11.76 ± 0.98 mg/L in effluent from the Sponge-MFC(C) and the MFC(C), resulting in removal efficiencies of $96.11 \pm 1.26\%$ and $94.31 \pm 1.82\%$, respectively. CEs in the Sponge-MFC(C) and the MFC(C) were $25.36 \pm 3.59\%$ and $15.57 \pm 5.73\%$, respectively, which indicated that a small proportion of glucose was used to generate power. CEs in this study were lower than those in MFCs fed by other organic carbon sources. Chae et al. [31] investigated the influence of the substrate type on performance of two-rectangular chambered MFCs and indicated that the MFC fed by acetate (72.3%), butyrate (43.0%) and propionate (36.0%)

were notably higher than glucose (15%). Acetate could directly generate electricity since it would be not degraded to other products. However, during the degradation process glucose was converted to acetone, acetate, ethanol and other products, which diverted electrons from the electricity production [32]. Additionally, other factors may also contribute to the decrease in CE, such as consumption of glucose by fermentation and methanogenesis, enrichment of non-electrochemically active bacteria, biomass generation, and neutral metabolites diffusing to the cathodic chamber [31, 33]. Moreover, the diffusion of oxygen from the cathodic chamber into the anodic chamber also caused the decline in CEs in MFCs since aerobic degradation of substrate reduced organic matter available for electricity production [34]. In contrast, attached biomass on the sponge in the Sponge-MFC(C) utilized the oxygen in the cathodic chamber for nitrification. As a result, less oxygen was diffused into the anodic chamber, giving rise to higher CE than the MFC(C).

Both voltage outputs and current densities were higher for the Sponge-MFC(C) (97.62 ± 4.73 mV and 0.16 ± 0.02 A/m², respectively) than those for the MFC(C) (70.65 ± 5.67 mV and 0.11 ± 0.03 A/m², respectively). The power densities of the Sponge-MFC(C) reached 30.50 ± 4.06 mW/m², while the MFC(C) had lower power densities of 15.98 ± 2.96 mW/m². These results were remarkably lower than those in other studies (> 52 mW/m²) with glucose as feed at a concentration of 1000 mg/L [33, 35]. In this study, feed water containing significantly lower influent COD concentration was employed as influent, which limited electricity generation and power generation by both MFCs.

3.3. Polarization curves, power curves and cathode impedance during the operational period

As shown in Fig. 2, the maximum power density in the Sponge-MFC(C) was obtained (32.58 mW/m²) at a current density of 0.18 A/m², while the corresponding value was lower in the MFC(C) at 17.40 mW/m² at a current density of 0.13 A/m². From the slope of the polarization curves, the Sponge-MFC(C) indicated lower internal resistance (47.40Ω) than the MFC(C) (65.35Ω).

Fig. 2.

EIS experiments were carried out at the end of experiment to compare the cathode performance between the Sponge-MFC(C) and MFC(C). Fig. 3 shows the Nyquist plot of cathode impedance spectra for the Sponge-MFC(C) and MFC(C) with equivalent circuits (insert in the same figure) through plotting the negative of the imaginary part of impedance (Z_{im}) vs the real part of impedance (Z_{re}). The cathode's impedance spectra were very consistent with an equal circuit, consisting of a solution resistance (R_s) in series with charge transfer resistance (R_{ct}) and a constant phase element (CPE) in parallel. The Nyquist plots for both MFCs demonstrated a semicircle without a straight line, suggesting the key role of R_{ct} and R_s in electrochemical reaction on the cathode, while there was no diffusionally limited electrochemical process [36], which were similar to the results documented by Zhang et al. [37]. R_{ct} and R_s in the MFC(C) (23 Ω and 7 Ω , respectively) were higher than those for the Sponge-MFC(C) (11 Ω and 4 Ω , respectively). A smaller R_{ct} for the Sponge-MFC(C) implied a faster electron-transfer rate between the cathode and the catholyte (suspended sludge in the cathodic chamber in this study) with enhanced catalytic activity of microorganisms on the cathode due to sponge addition [38]. The relatively lower R_s than R_{ct} for the MFC systems indicated that the ohmic limitation had less impact on cathode performance, while charge transfer was a rate-limiting step.

In this study, charge transfer (e.g. protons) was mainly affected by activated sludge concentration as it was positively associated with sludge viscosity which adversely influenced the transfer rate. MLSS concentrations in the MFC(C) were 6.3321 ± 0.2518 g/L, while the sponge could create a balance between suspended sludge and attached biomass on the sponge, therefore reducing suspended sludge concentration in the Sponge-MFC(C) (5.2435 ± 0.1826 g/L) and further decreasing R_s . It suggested that positive impacts of the sponge on the cathodic impedance could greatly offset its negative effects (non-conductive carriers may inhibit the charge transfer). Effects of other sludge

properties (e.g. extracellular polymeric substances (EPS), soluble microbial products (SMP)) on R_{ct} will be investigated in a future study. The capacitance of the cathode obtained from constant phase element (CPE) value was 352.38 mF for the Sponge-MFC(C), which was higher than that for the MFC(C) at 234.92 mF. It indicated a less active surface area and more severe pore clogging on the cathode occurred in the MFC(C) when compared to those for the Sponge-MFC(C) [39]. This could be ascribed to the excessive growth of biomass on the cathode in the MFC(C). Conversely, the sponge in the Sponge-MFC(C) scoured the cathode surface, which maintained a larger active surface area of the cathode, resulting in higher capacitance. Hence, more reaction sites on the cathode available for oxidant reduction were obtained in the Sponge-MFC(C), leading to higher cathodic reaction rate and power outputs [40].

Fig. 3.

To investigate the biomass on the cathode in both MFC systems, a mass balance calculation was employed in the cathodic chamber during 90 days of operation. The total biomass in the cathodic chamber is the sum of initial suspended sludge, initial attached biomass on the sponge, net growth of suspended sludge and attached biomass on the sponge over the experimental period, and attached biomass growth on the cathode. The amount of biomass on the cathode can be calculated by the following equation:

$$\text{For MFC(C): } MLSS_{in,M} \times V + \Delta MLSS_{g,M} \times V + SS_{C,M} = \int_0^{90} MLSS_{M(t)} dt \times Q \times 20/24 \quad (4)$$

$$\text{Sponge-MFC(C): } MLSS_{in,S} \times V + \Delta MLSS_{g,S} \times V + SS_{C,S} + SS_{SP} \times V_{SP} + \Delta SS_{SP} \times V_{SP} = \int_0^{90} MLSS_{S(t)} dt \times Q \times 20/24 \quad (5)$$

where the subscripts S and M standard for the Sponge-MFC(C) and the MFC(C), $MLSS_{in}$ is the initial suspended biomass concentration (g/L), $\Delta MLSS_g$ and ΔSS_{SP} are average net growth of mixed liquor suspended biomass concentrations (g/L·d) and attached biomass (g/L sponge) over the

operational days (90 days), respectively, V is the working volume of the cathodic chamber (L), SS_C is the amount of biomass on and inside the cathode (g), SS_{SP} is the concentration of biomass from sponge (g/L sponge), V_{SP} is the sponge volume in the cathodic chamber (L), $MLSS_{M(t)}$ and $MLSS_{S(t)}$ are the concentrations of biomass which were washed out from the cathodic chamber (g/L) of the MFC(C) and the Sponge-MFC(C) at different operational day, respectively, t is the operational day (d), and Q is the flow rate of the cathodic chamber (L/h).

$$MLSS_{M(t)} = (W_{M2(t)} - W_{M1(t)}) / a_{M(t)} \quad (6)$$

$$MLSS_{S(t)} = (W_{S2(t)} - W_{S1(t)}) / a_{S(t)} \quad (7)$$

where $W_{2(t)}$ is the weight of biomass and filter paper (g) at the operational day (t), $W_{1(t)}$ is the weight of filter paper (g) at the operational day (t), $a(t)$ is the volume of biomass samples (L) at the operational day (t).

In this study, the effective working volume of the cathodic chamber is 3 L. The filling ratio of the sponge is 2%. The flow rate was 0.25 L/h. The operational duration per 24 h (per day) is 20 h. The initial suspended sludge concentrations for the Sponge-MFC(C) and the MFC(C) were 3.0105 ± 0.1021 and 2.9816 ± 0.1327 g/L, respectively, while the corresponding concentrations increased to 5.2435 ± 0.1826 and 6.3321 ± 0.2518 g/L after 90 days, yielding the average net growth of suspended biomass was 2.2330 and 3.3505 g/L, also respectively. Sponge initially possessed 16.9672 g/L sponge of the attached biomass, which increased to 18.0647 g/L sponge when the experiment ended. As a consequence, the attached biomass production was 1.0975 g/L sponge through the whole experiment. Thus a larger amount of biomass was accumulated on the cathode of the MFC (10.6819 ± 0.8636 g) than that of the Sponge-MFC (7.7593 ± 0.3172 g). These results confirmed more abundant biomass was present on the cathode in the MFC(C) compared to the Sponge-MFC(C).

3.4. Nutrient removal of the Sponge-MFC and MFC during the operational period

3.4.1. Nitrogen removal

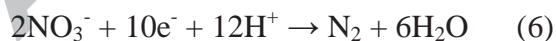
The operation of both MFC systems was conducted under the closed- and open-circuit modes. Here the objective was to investigate the contribution of electrochemical reaction and biological process to nitrogen removal. Table 1 shows concentrations of $\text{NH}_4\text{-N}$, $\text{NO}_3\text{-N}$, $\text{NO}_2\text{-N}$ and T-N from the effluent of the Sponge-MFC and the MFC under the closed-circuit and open-circuit conditions.

Table 1.

At the open-circuit mode, DO concentrations in the cathodic chamber were kept at relatively high levels of 4.68 ± 0.75 and 4.35 ± 0.59 mg/L for the Sponge-MFC(O) and the MFC(O), respectively. $\text{NH}_4\text{-N}$ removals for the Sponge-MFC(O) and the MFC(O) were mainly found in the cathodic chamber, with effluent concentrations of 8.63 ± 0.29 and 15.09 ± 1.56 mg/L at removal rates of 0.152 ± 0.023 and 0.136 ± 0.035 kg/(m^3 TRV·d), respectively. It led to higher $\text{NH}_4\text{-N}$ removals of $88.01 \pm 1.53\%$ in the Sponge-MFC(O) than $79.04 \pm 2.67\%$ in the MFC(O), demonstrating that $\text{NH}_4\text{-N}$ was mainly eliminated in the cathodic chamber. In this study, the synthetic wastewater containing high $\text{NH}_4\text{-N}$ loading required higher DO levels for nitrification. Thus the limited oxygen penetration into the cathodic biofilm prompted SND process on the cathode [41]. It resulted in T-N removal of $57.90 \pm 2.24\%$ in the MFC(O) with effluent $\text{NO}_3\text{-N}$ and $\text{NO}_2\text{-N}$ concentrations of 13.36 ± 2.54 and 1.86 ± 1.03 mg/L at removal rates of 0.100 ± 0.003 kg N/(m^3 TRV·d), respectively. In the Sponge-MFC(O), sponge addition improved $\text{NH}_4\text{-N}$ removal due to the enrichment of ammonium oxidizing bacteria (AOB) and nitrite oxidizing bacteria (NOB) on the acclimatized sponge. Additionally, the sponge created an aerobic state at its outer layer and an anoxic one at the inner layer [42, 43]. Consequently, the effluent $\text{NO}_3\text{-N}$ and $\text{NO}_2\text{-N}$ concentrations from the cathodic chamber were detected at lower levels for the

Sponge-MFC(O) (10.35 ± 1.43 and 2.27 ± 0.17 mg/L, respectively), resulting in higher TN removals of $70.49 \pm 2.59\%$ at removal rates of 0.122 ± 0.002 kg/(m³ TRV·d).

When operating under the closed-circuit mode, NH₄-N concentrations in the anodic effluent for the Sponge-MFC(C) and the MFC(C) were similar (45.63 ± 2.57 and 48.49 ± 3.64 mg/L, respectively). The final NH₄-N concentrations in the effluent from the Sponge-MFC(C) were significantly lower (2.85 ± 0.41 mg/L) with higher removal efficiencies of $96.04 \pm 1.37\%$ compared to the MFC(C) (14.36 ± 1.31 mg/L and $80.06 \pm 2.18\%$, respectively). NH₄-N removal rates reached 0.166 ± 0.032 and 0.138 ± 0.057 kg N/(m³ TRV·d) for the Sponge-MFC(C) and the MFC(C), respectively. The effluent from the cathodic chamber of the Sponge-MFC(C) at DO concentrations of 4.47 ± 0.28 mg/L contained no appreciable levels of NO₃-N (0.12 ± 0.03 mg/L), while a considerable increase in NO₃-N was observed in the effluent from the cathodic chamber of the MFC(C) at 3.05 ± 0.15 mg/L (DO, 4.36 ± 0.55 mg/L). The effluent NO₂-N concentrations in both MFC systems were low at 0.02 ± 0.01 mg/L. T-N removal efficiencies in the Sponge-MFC(C) were $90.73 \pm 1.87\%$, higher than those for the MFC(C) at $68.85 \pm 2.98\%$ at removal rates of 0.165 ± 0.018 and 0.131 ± 0.029 kg N/m³ TRV·d, respectively. In this study, NH₄-N elimination in the anodic chamber could be ascribed to NH₄⁺ going through PEM and then entering the cathodic chamber due to NH₄-N concentration gradient between the anodic and cathodic chambers. Apart from this the charge imbalance between the two chambers contributed to the NH₄-N decline. The protons produced by the anodic chamber were consumed by the cathode as shown in Eq. (6) [44] and created a charge imbalance. Thus the charge transfer as a result of electricity generation could maintain the charge balance between two chambers.



Since pH near the cathode was detected at 8.23 ± 0.42 in the Sponge-MFC(C) and 8.01 ± 0.58 in the MFC(C), the NH₄-N volatilization may also take place adjacent to the cathode [45]. Conversely, the loop-operated MFC could prompt the additional transfer of protons generated by anaerobic oxidation of

carbon sources in the anodic chamber to the cathodic chamber. This process can be achieved via the liquid stream [7]. Thus, the pH values in this study were maintained at relatively constant levels in the cathodic chambers (7.05 ± 0.25 for the Sponge-MFC(C) and 7.09 ± 0.32 for the MFC(C)). It reduced chemical requirements and costs (sodium bicarbonate).

There were significantly higher TN removals with considerably smaller $\text{NO}_3\text{-N}$ and $\text{NO}_2\text{-N}$ contents in the closed-circuit MFC systems than the open-circuit systems. This suggested that the bioelectrochemical denitrification process on the cathode could further improve nitrogen removal when closing the circuit. During the bioelectrochemical denitrification process, denitrifying microorganisms located at the cathode biofilm's inner layer employed the electrons provided by the cathode to reduce both $\text{NO}_3\text{-N}$ and $\text{NO}_2\text{-N}$ [8, 46]. Overall, the biological nitrogen removal process (i.e. nitrification and SND) coupled with the bioelectrochemical denitrification process led to the removal of nitrogen in the Sponge-MFC(C) and the MFC(C). The contributions of bioelectrochemical denitrification to nitrogen removal in the Sponge-MFC(C) and the MFC(C) were 26.06% and 23.62%, respectively.

In order to elucidate the electrochemical reactions on the cathode surface, cyclic voltammetry analyses were undertaken for the cathodes in the cathodic chambers with and without sponge at the experiment's completion. As shown in Fig. 4, when the cathode was fed with a medium containing $\text{NO}_3\text{-N}$, the Sponge-MFC(C) exhibited one oxidation peak and one reduction peak (approximately -0.017 V (vs Ag/AgCl) and -0.35 V (vs Ag/AgCl), respectively) compared to the MFC(C) with one reduction peak (-0.27 V (vs Ag/AgCl)). It could be inferred that $\text{NO}_3\text{-N}$ reduction occurred at -0.35 V and -0.27 V (vs Ag/AgCl for the Sponge-MFC(C) and the MFC(C), respectively). In this study, the electrochemical response decreased on the cathode in the MFC(C) due to excessive growth of biomass on the cathode, resulting in a less active surface area for transfer of electrons and oxygen, which discouraged cathodic reaction (bioelectrochemical denitrification in this study). In contrast, the cathode

of the Sponge-MFC(C) indicated higher and more stable electrochemical activity for $\text{NO}_3\text{-N}$ reduction by enrichment of denitrifying bacteria.

Fig. 4.

3.4.2. FISH and electrochemical analyses of the cathode and sponge

Nitrifying and denitrifying bacteria of the cathode and sponge were examined using FISH. Figs. 5(a)-(d) display CLSM images of nitrifying bacteria in the attached biomass collected from the outer layer of the cathode in the Sponge-MFC and the MFC in closed-circuit and open-circuit modes. The community fractions of NOB were the highest at the outer layer of the biofilm in the Sponge-MFC(C) compared to the Sponge-MFC(O), the MFC(C) and the MFC(O) ($65.3 \pm 2.6\%$, $43.6 \pm 3.7\%$, $38.7 \pm 2.9\%$ and $26.7 \pm 2.2\%$, respectively). However, all of the MFC systems contained small proportions of AOB ($6.5 \pm 0.3\%$ (Sponge-MFC(C)), $10.6 \pm 1.1\%$ (Sponge-MFC(O)), $14.8 \pm 1.3\%$ (MFC(C)), and $13.5 \pm 1.6\%$ (MFC(O)). Suggested here is the possibility that closed-circuit operation favored the growth of NOB at the outer layer of the cathodic biofilm, which prompted the conversion of $\text{NH}_4\text{-N}$ into $\text{NO}_3\text{-N}$ at high DO concentration. Furthermore, the presence of sponge could maintain higher percentages and activity of NOB in the Sponge-MFC(C) and the Sponge-MFC(O). At the cathode's interior layer (Supplementary Fig. S1), *Paracoccus* genus and *Pseudomonas* spp. were detected as the dominant species in the Sponge-MFC(C) ($28.3 \pm 2.4\%$ and $34.6 \pm 1.5\%$, respectively), which were higher than those in the MFC(C) ($18.1 \pm 1.6\%$ and $16.5 \pm 1.4\%$, respectively) (Figs. 6(a) and (b)). The SEM results (Supplementary Fig. S2) confirmed *Paracoccus* genus (micrococcus-shaped) and *Pseudomonas* spp. (rod-shaped) were more abundant in the Sponge-MFC(C) than in the MFC(C), which were similar to the findings reported by Zhang et al. [27]. These species could employ electrons from the cathode to reduce $\text{NO}_3\text{-N}$ [27, 47]. Furthermore, a larger proportion of the total biomass area was identified in the Sponge-MFC(C) ($13.2 \pm 1.4\%$ and $10.5 \pm 1.3\%$, respectively) by probe LGC354 and probe GFX1223

belonging to Phylum Firmicutes and Phylum Chloroflexi than that in the MFC(C) ($8.3 \pm 0.8\%$ and $4.3 \pm 0.4\%$, respectively). Phylum Firmicutes was associated with $\text{NO}_2\text{-N}$ reduction, while Phylum Chloroflexi contributed to $\text{NO}_3\text{-N}$ reduction [48, 49]. However, these bacteria as mentioned above were not that much evident in the MFC systems when opening the circuit. On the other hand, Gammaproteobacteria and Alphaproteobacteria for $\text{NO}_3\text{-N}$ reduction [44] in the Sponge-MFC(O) accounted for $25.3 \pm 2.1\%$ and $20.2 \pm 1.8\%$ of the total microbial community, respectively (Supplementary Fig. S1). These percentages were similar to those in the MFC(O) ($22.3 \pm 2.1\%$ and $18.4 \pm 1.7\%$, respectively). Smaller amounts of Gammaproteobacteria and Alphaproteobacteria were found in the Sponge-MFC(C) ($5.1 \pm 0.5\%$ and $6.3 \pm 0.6\%$, respectively) and the MFC(C) ($6.4 \pm 0.6\%$ and $8.5 \pm 0.8\%$, respectively). These results indicated that at the closed-circuit mode, the addition of sponge could enhance the diversity of denitrifying bacteria and promote the growth of *Paracoccus* genus and *Pseudomonas* spp. on the cathode. Moreover, the presence of nitrifying bacteria at the outer layer and denitrifying bacteria at the inner layer of the cathode promoted electrochemical denitrification and SND processes.

Fig. 5.

Fig. 6.

As shown in Table 2, the presence of sponge stimulated the growth of AOB and NOB in the Sponge-MFC systems regardless of circuit mode (Supplementary Fig. S3). Although the Sponge-MFC(O) possessed larger amounts of Gammaproteobacteria and Alphaproteobacteria, more diverse populations of denitrifying bacteria were detected in the Sponge-MFC(C). It can be argued that sponge addition could enhance the SND process in the MFC when operating under closed-circuit conditions.

Table 2.

3.4.3. Phosphorus removal

During the open-circuit operation, $\text{PO}_4\text{-P}$ concentrations in the anodic effluent from the Sponge-MFC(O) and the MFC(O) were higher (7.73 ± 0.76 and 7.69 ± 0.82 mg/L, respectively) than those in the influent owing to anaerobic phosphorus release in the anodic chamber using glucose as carbon source. The MFC(O) revealed low $\text{PO}_4\text{-P}$ removal of $38.82 \pm 7.96\%$ with effluent $\text{PO}_4\text{-P}$ concentrations of 4.16 ± 1.64 mg/L, indicating that $\text{PO}_4\text{-P}$ removal was mainly achieved through phosphorus uptake by phosphate accumulating organisms (PAOs) under aerobic conditions in the cathodic chamber [50]. Higher $\text{PO}_4\text{-P}$ removal efficiencies of $57.74 \pm 8.62\%$ in the Sponge-MFC(O) were due to the formation of oxic/anoxic zones on the sponge which improved phosphorus uptake.

It has been reported that phosphorus removal could be achieved by the precipitation of phosphate salts resulting from the alkaline cathode liquor [11, 12]. pH values in the proximity of the cathode of the Sponge-MFC(C) and the MFC(C) were higher (> 8) than those at other sites in the cathodic chamber, which was favorable for struvite formation on the cathode [51]. Therefore, effects of precipitation on phosphorus removal and recovery were also taken into account in this study. In order to verify the presence of the struvite (or $\text{MgNH}_4\text{PO}_4 \cdot 6\text{H}_2\text{O}$, MAP), more analyses were done on the precipitations on the cathodes of both MFCs. XRD patterns of the precipitates on the cathode in the Sponge-MFC(C) and MFC(C) (Figs. 7(a) and (b)) were similar to those of MAP standard (JCPDS 15-0762). Moreover, the qualitative analysis on MAP precipitates through a dissolution method showed that Mg^{2+} and PO_4^{3-} concentrations of the precipitates from the Sponge-MFC(C) were 9.77 and 40.6 mg/L, respectively, while the corresponding values in the MFC(C) were lower at 5.86 and 25.3 mg/L, respectively. In addition, the precipitates of the Sponge-MFC(C) and the MFC(C) possessed NH_4^+ levels at 7.41 and 4.81 mg/L, respectively.

It could be inferred from these results that the molar ratio of $[\text{Mg}^{2+}]$: $[\text{NH}_4^+]$: $[\text{PO}_4^{3-}]$ in the precipitation was 1:1.07:1.05, which agreed well with the theoretical molar ratio of Mg: N: P to form struvite at 1:1:1 when compared to the molar ratio in the MFC(C) (1:1.16:1.09). These results implied

the appearance of the MAP on the cathode surface was more significant in the Sponge-MFC(C). SEM analyses (Fig. S4 in Supporting information) showed that the morphology of the MAP precipitates in both MFCs were similar to the orthorhombic crystals [52, 53]. These results suggested the formation of MAP on the cathode in both MFCs at closed-circuit mode. The comparison in $\text{PO}_4\text{-P}$ removals between MFCs at the open- and closed-circuit modes demonstrated that the MAP formation accounted for 26.32% and 15.15%, respectively, of $\text{PO}_4\text{-P}$ removals for the Sponge-MFC(C) and the MFC(C). Overall, both biological phosphorus removal and MAP formation were responsible for phosphorus removal in this study, eliminating $\text{PO}_4\text{-P}$ by $82.06 \pm 1.21\%$ and $53.97 \pm 2.32\%$ for the Sponge-MFC(C) and the MFC(C), respectively.

Fig. 7.

4. Conclusions

This study investigated the performance of the Sponge-MFC and the MFC when treating low C/N wastewater. In comparison to the MFC(C), sponge addition increased voltage outputs, and current and power densities, while reducing R_{ct} and R_s . The Sponge-MFC(C) stimulated the growth of diverse denitrifying bacteria, which further enhanced nitrogen removal through the sponge's SND process and the cathode together with the bioelectrochemical denitrification process on the cathode. The combined processes of biological phosphorus removal and phosphorus recovery as struvite led to a considerable amount of phosphorus being removed in the Sponge-MFC(C). Therefore it can be confirmed that sponge addition in the MFC system was a feasible technology for treating low C/N ratio wastewater.

Acknowledgements

This study is mainly supported by Postdoctoral Science Foundation of China [No. 2016M601268], the National Natural Science Foundation of China [No. 51578375, 51378349], and Science and Technology Planning Project of Tianjing, China [No. 15PTSJYC00230, 14ZCDGSF00128]. The

authors are also grateful for the research collaboration between University of Technology and Tianjin Polytechnic University.

References

- [1] G. Mannina, M. Capodici, A. Cosenza, D. Di Trapani, Carbon and nutrient biological removal in a University of Cape Town membrane bioreactor: Analysis of a pilot plant operated under two different C/N ratios, *Chem. Eng. J.* 296 (2016) 289–299.
- [2] Y. Guo, Y. Peng, B. Wang, B. Li, M. Zhao, Achieving simultaneous nitrogen removal of low C/N wastewater and external sludge reutilization in a sequencing batch reactor, *Chem. Eng. J.* 306 (2016) 925–932.
- [3] J. Meng, J. Li, J. Li, P. Antwi, K. Deng, C. Wang, G. Buelna, Nitrogen removal from low COD/TN ratio manure-free piggery wastewater within an upflow microaerobic sludge reactor, *Bioresour. Technol.* 198 (2015) 884–890.
- [4] M. Zhang, C. Wang, Y. Peng, S. Wang, F. Jia, W. Zeng, Organic substrate transformation and sludge characteristics in the integrated anaerobic anoxic oxic–biological contact oxidation (A^2/O –BCO) system treating wastewater with low carbon/nitrogen ratio, *Chem. Eng. J.* 283 (2016) 47–57.
- [5] S. Cao, R. Du, M. Niu, B. Li, N. Ren, Y. Peng, Integrated anaerobic ammonium oxidization with partial denitrification process for advanced nitrogen removal from high-strength wastewater, *Bioresour. Technol.* 221 (2016) 37–46.
- [6] J. Meng, J. Li, J. Li, P. Antwi, K. Deng, C. Wang, G. Buelna, Nitrogen removal from low COD/TN ratio manure-free piggery wastewater within an upflow microaerobic sludge reactor *Bioresour. Technol.* 198 (2015) 884–890.
- [7] B. Virdis, K. Rabaey, Z. Yuan, J. Keller, Microbial fuel cells for simultaneous carbon and nitrogen removal, *Water Res.* 42 (2008) 3013–3024.

- [8] B. Virdis, K. Rabaey, R.A. Rozendal, Z. Yuan, J. Keller, Simultaneous nitrification, denitrification and carbon removal in microbial fuel cells, *Water Res.* 44 (2010) 2970–2980.
- [9] F. Zhang, Z. He, Integrated organic and nitrogen removal with electricity generation in a tubular dual-cathode microbial fuel cell, *Process Biochem.* 47 (2012) 2146–2151.
- [10] G. Zhang, H. Zhang, C. Zhang, G. Zhang, F. Yang, G. Yuan, F. Gao, Simultaneous nitrogen and carbon removal in a single chamber microbial fuel cell with a rotating biocathode, *Process Biochem.* 48 (2013) 893–900.
- [11] Q. Tao, J. Luo, J. Zhou, S. Zhou, G. Liu, R. Zhang, Effect of dissolved oxygen on nitrogen and phosphorus removal and electricity production in microbial fuel cell, *Bioresour. Technol.* 164 (2014) 402–407.
- [12] K. Hirooka, O. Ichihashi, Phosphorus recovery from artificial wastewater by microbial fuel cell and its effect on power generation, *Bioresour. Technol.* 137 (2013) 368–375.
- [13] G.L. Zang, , G.P. Sheng, , W.W. Li, Z.H. Tong, , R.J. Zeng, C. Shi, H.Q. Yu, Nutrient removal and energy production in a urine treatment process using magnesium ammonium phosphate precipitation and a microbial fuel cell technique, *Phys. Chem. Chem. Phys.* 14 (2012) 1978–1984.
- [14] J.L. Shore, W.S. M'Coy, C.K. Gunsch, M.A. Deshusses, Application of a moving bed biofilm reactor for tertiary ammonia treatment in high temperature industrial wastewater, *Bioresour. Technol.* 112 (2012) 51–60.
- [15] F.A. Almomani, R. Delatolla, B. Örmeci, Field study of moving bed biofilm reactor technology for post-treatment of wastewater lagoon effluent at 1°C, *Environ. Technol.* 35 (2014) 1596–1604.
- [16] M.K.H. Winkler, J. Yang, R. Kleerebezem, E. Plaza, J. Trela, B. Hultman, M.C.M. van Loosdrecht, Nitrate reduction by organotrophic Anammox bacteria in a nitrification/ anammox granular sludge and a moving bed biofilm reactor, *Bioresour. Technol.* 114 (2012) 217–223.

- [17] L. Chu, J. Wang, Nitrogen removal using biodegradable polymers as carbon source and biofilm carriers in a moving bed biofilm reactor, *Chem. Eng. J.* 170 (2011) 220–225.
- [18] Q. Feng, Y. Wang, T. Wang, H. Zheng, L. Chu, C. Zhang, H. Chen, X. Kong, X.H. Xing, Effects of packing rates of cubic-shaped polyurethane foam carriers on the microbial community and the removal of organics and nitrogen in moving bed biofilm reactor, *Bioresour. Technol.* 117 (2012) 201–207.
- [19] J.W. Lim, P.E. Lim, C.E. Seng, Enhancement of nitrogen removal in moving bed sequencing batch reactor with intermittent aeration during REACT period, *Chem. Eng. J.* 197 (2012) 199–203.
- [20] H.H. Ngo, W. Guo, W. Xing, Evaluation of a novel sponge-submerged membrane bioreactor (SSMBR) for sustainable water reclamation, *Bioresour. Technol.* 99 (2008) 2429–2435.
- [21] L.J. Deng, W.S. Guo, H.H. Ngo, X. Zhang, X.C. Wang, Q. Zhang, R. Chen, New functional biocarriers for enhancing the performance of a hybrid moving bed biofilm reactor-membrane bioreactor system, *Bioresour. Technol.* 208 (2016) 87–93.
- [22] B.E. Logan, *Microbial fuel cells*, John Wiley & Sons, Inc., Hoboken, N.J., U.S.A., 2007.
- [23] K. Chung, I. Fujiki, S. Okabe, Effect of formation of biofilms and chemical scale on the cathode electrode on the performance of a continuous two-chamber microbial fuel cell, *Bioresour. Technol.* 102 (2011) 355–360.
- [24] B. Xie, B. Liu, Y. Yi, L. Yang, D. Liang, Y. Zhu, H. Liu, Microbiological mechanism of the improved nitrogen and phosphorus removal by embedding microbial fuel cell in anaerobic–anoxic–oxic wastewater treatment process, *Bioresour. Technol.* 207 (2016) 109–117.
- [25] O. Ichihashi, K. Hirooka, Removal and recovery of phosphorus as struvite from swine wastewater using microbial fuel cell, *Bioresour. Technol.* 114 (2012) 303–307.

- [26] X.D. Hao, C.C. Wang, L. Lan, M.C.M. van Loosdrecht, Struvite formation, analytical methods and effects of pH and Ca^{2+} , *Water Sci. Technol.* 58 (2008) 1687-1692.
- [27] G. Zhang, H. Zhang, Y. Ma, G. Yuan, F. Yang, R. Zhang, Membrane filtration biocathode microbial fuel cell for nitrogen removal and electricity generation, *Enzyme Microb. Technol.* 60 (2014) 56–63.
- [28] R.I. Amann, In Situ Identification of Micro-organisms by Whole Cell Hybridization with rRNA-Targeted Nucleic Acid Probes, in: A.D.L. Akkermans, J.D. Van Elsas, F.J. De Bruijn (Eds.), *Molecular Microbial Ecology Manual*, Kluwer Academic Publishers, The Netherlands, 1995. pp. 1–15.
- [29] H. Daims, S. Lucker, M. Wagner, Daime, a novel image analysis program for microbial ecology and biofilm research, *Environ. Microbiol.* 8 (2006) 200–213.
- [30] H.H. Ngo, M.C. Nguyen, N.G. Sangvikar, T.T.L. Hoang, W.S. Guo, Simple approaches towards the design of an attached-growth sponge bioreactor (AGSB) for wastewater treatment and reuse, *Water Sci. Technol.* 54 (2006) 191–197.
- [31] K.J. Chae, M.J. Choi, J.W. Lee, K.Y. Kim, I.S. Kim, Effect of different substrates on the performance, bacterial diversity, and bacterial viability in microbial fuel cells, *Bioresour. Technol.* 100 (2009) 3518-3525.
- [32] Y. Sharma, B. Li, The variation of power generation with organic substrates in single-chamber microbial fuel cells (SCMFCs), *Bioresour. Technol.* 101 (2010) 1844-1850.
- [33] Y. Zhang, B. Min, L. Huang, I. Angelidaki, Electricity generation and microbial community response to substrate changes in microbial fuel cell, *Bioresour. Technol.* 102 (2011) 1166-1173.
- [34] N. Lu, S.G. Zhou, L. Zhuang, J.T. Zhang, J.R. Ni, Electricity generation from starch processing wastewater using microbial fuel cell technology, *Biochem. Eng. J.* 43 (2009) 246–251.

- [35] B. Min, B. Logan, Continuous electricity generation from domestic wastewater and organic substrates in a flat plate microbial fuel cell, *Environ. Sci. Technol.* 38 (2004) 5809–5814.
- [36] E. Katz, I. Willner, Probing biomolecular interactions at conductive and semiconductive surfaces by impedance spectroscopy: routes to impedimetric immunosensors, DNA-Sensors, and Enzyme Biosensors, *Electroanalysis* 15 (2003) 913-947.
- [37] Y. Zhang, S. Jian, B. Hou, Y. Hu, Performance improvement of air-cathode single-chamber microbial fuel cell using a mesoporous carbon modified anode, *J. Power Sources* 196 (2011) 7458-7464.
- [38] B. Hou, Y. Hu, J. Sun, Performance and microbial diversity of microbial fuel cells coupled with different cathode types during simultaneous azo dye decolorization and electricity generation, *Bioresour. Technol.* 111 (2012) 105-110.
- [39] F. Zhang, D. Pant, B.E. Logan, Long-term performance of activated carbon air cathodes with different diffusion layer porosities in microbial fuel cells, *Biosens. Bioelectron.* 30 (2011) 49-55.
- [40] H. Rismani-Yazdi, S.M. Carver, A.D. Christy, O.H. Tuovinen, Cathodic limitations in microbial fuel cells: an overview, *J. Power Sources* 180 (2008) 683–694.
- [41] Y. Mao, X. Quan, H. Zhao, Y. Zhang, S. Chen, T. Liu, W. Quan, Accelerated startup of moving bed biofilm process with novel electrophilic suspended biofilm carriers, *Chem. Eng. J.* 315 (2017) 364-372.
- [42] W. Guo, H.H. Ngo, S. Vigneswaran, W. Xing, P. Goteti, A novel sponge submerged membrane bioreactor (SSMBR) for wastewater treatment and reuse, *Sep. Sci. Technol.* 43 (2008) 273–285.
- [43] T.T. Nguyen, H.H. Ngo, W.S. Guo, J.X. Li, A. Listowski, Effects of sludge concentrations and different sponge configurations on the performance of a sponge-submerged membrane bioreactor, *Appl. Biochem. Biotechnol.* 167 (2012) 1678–1687.

- [44] C. Jiang, Q. Yang, D. Wang, Y. Zhong, F. Chen, X. Li, G. Zeng, X. Li, M. Shang, Simultaneous perchlorate and nitrate removal coupled with electricity generation in autotrophic denitrifying biocathode microbial fuel cell, *Chem. Eng. J.* 308 (2017) 783–790.
- [45] Y. Tian, W. He, X. Zhu, W. Yang, N. Ren, B.E. Logan, Energy efficient electrocoagulation using an air-breathing cathode to remove nutrients from wastewater, *Chem. Eng. J.* 292 (2016) 308-314.
- [46] X. Zhang, F. Zhu, L. Chen, Q. Zhao, G. Tao, Removal of ammonia nitrogen from wastewater using an aerobic cathode microbial fuel cell, *Bioresour. Technol.* 146 (2013) 161-168.
- [47] W. Su, L. Zhang, D. Li, G. Zhan, J. Qian, Y. Tao, Dissimilatory nitrate reduction by *Pseudomonas alcaliphila* with an electrode as the sole electron donor, *Biotechnol. Bioeng.* 109 (2012) 2904-2910.
- [48] S. Kondaveeti, S.H. Lee, H.D. Park, B. Min, Bacterial communities in a bioelectrochemical denitrification system: The effects of supplemental electron acceptors, *Water Res.* 51 (2014) 25-36.
- [49] K.C. Wrighton, B. Virdis, P. Clauwaert, S.T. Read, R.A. Daly, N. Boon, Y. Piceno, G.L. Andersen, J.D. Coates, K. Rabaey, Bacterial community structure corresponds to performance during cathodic nitrate reductions, *The ISME Journal* 4 (2010) 1443–1455.
- [50] T. Liu, X. Chen, X. Wang, S. Zheng, L. Yang, Highly effective wastewater phosphorus removal by phosphorus accumulating organism combined with magnetic sorbent MFC@La(OH)₃, *Chem. Eng. J.* 335 (2018) 443–449.
- [51] P.T. Kelly, Z. He, Nutrients removal and recovery in bioelectrochemical systems: a review, *Bioresour. Technol.* 153 (2014) 351-360.
- [52] K.S. Le Corre, E. Valsami-Jones, P. Hobbs, S.A. Parsons, Impact of reactor operation on success of struvite precipitation from synthetic liquors, *Environ. Technol.* 28 (2007) 1245-1256.

- [53] K.S. Le Corre, E. Valsami-Jones, P. Hobbs, S.A. Parsons, Phosphorus recovery from wastewater by struvite crystallization: a review, *Critical Reviews in Environmental Science and Technology* 39 (2009) 433-477.

ACCEPTED MANUSCRIPT

Figure captions

Fig. 1. Experimental set-up of the Sponge-MFC

Fig. 2. Power density curves and polarization curves of the Sponge-MFC(C) and the MFC(C)

Fig. 3. Nyquist plot of cathode impedance spectra for the Sponge-MFC(C) and the MFC(C)

Fig. 4. Cyclic voltammogram of the cathode taken from the Sponge-MFC(C) and the MFC(C) with $\text{NO}_3\text{-N}$ medium (the same as those in the feed)

Fig. 5. CLSM images of nitrifying bacteria in the attached biomass collected from the outer layer of cathode in the Sponge-MFC and the MFC at the closed-circuit and open-circuit modes. (a) Sponge-MFC at the closed-circuit mode, (b) MFC at the closed-circuit mode, (c) Sponge-MFC at the open-circuit mode and (d) MFC at the open-circuit mode. FISH with CY-3 labeled AOBmix (red) probes, CY5-labeled NOBmix (blue) probes and FITC-labeled EUBmix (green) probes.

Fig. 6. Percentages of different denitrifying bacteria in biofilm inside the cathode of the Sponge-MFC(C) and MFC(C) as determined by FISH

Fig. 7. XRD patterns of precipitates on the cathode of the Sponge-MFC(C) (a) and the MFC(C) (b)

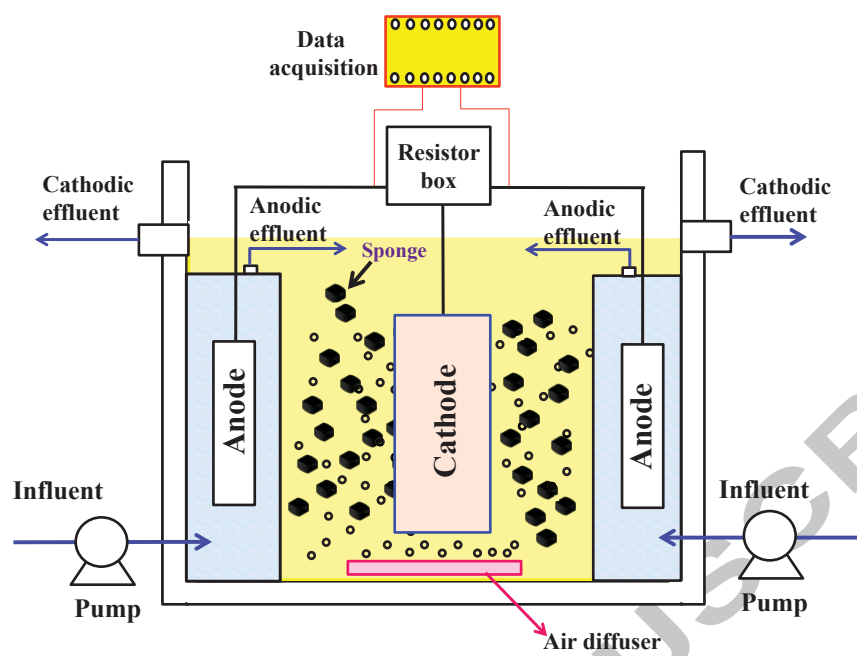


Fig. 1.

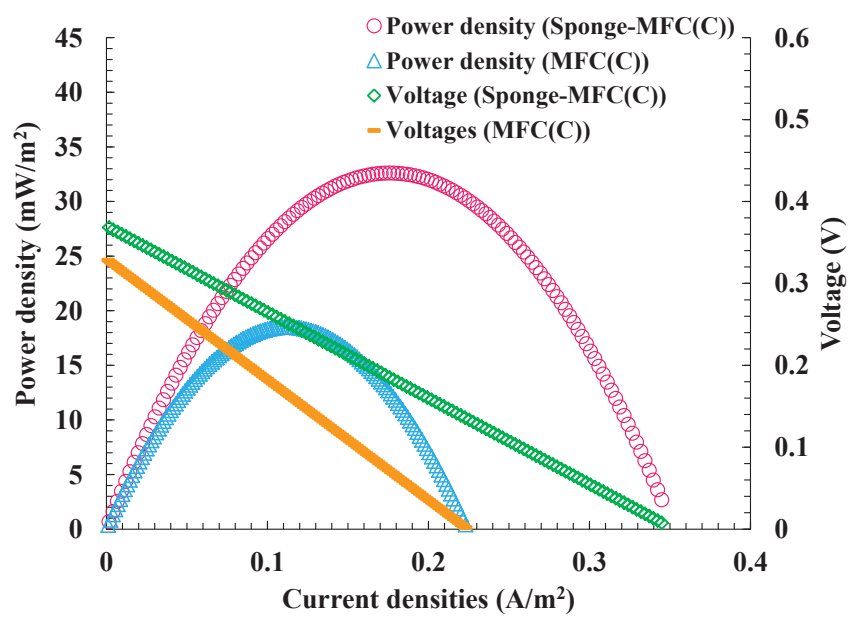


Fig. 2.

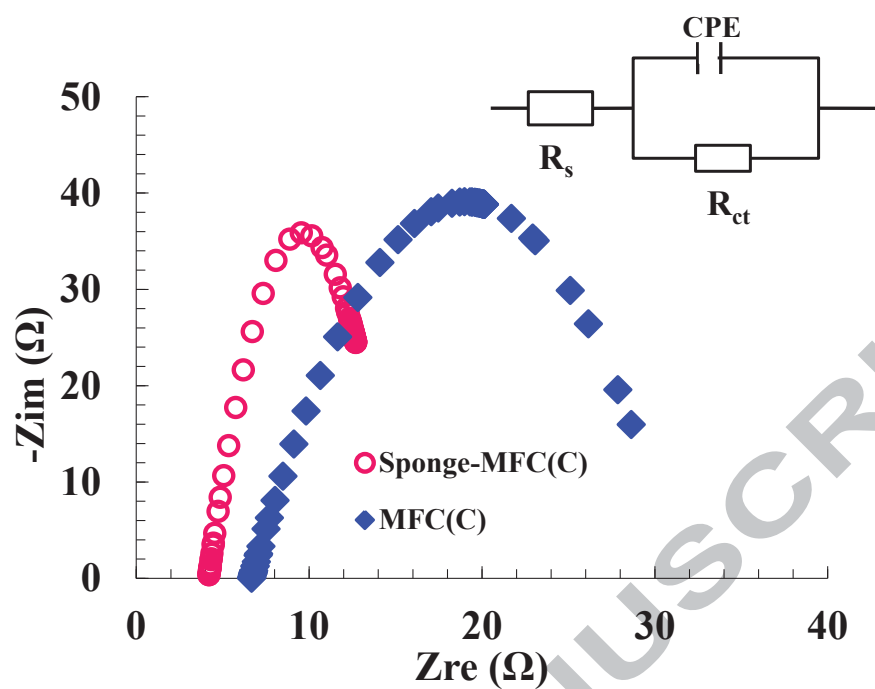


Fig. 3.

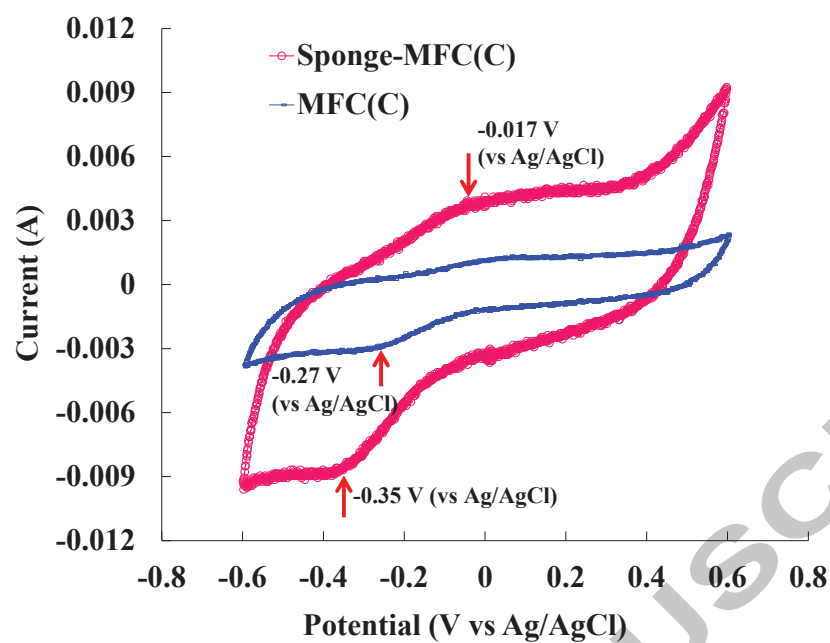


Fig. 4.

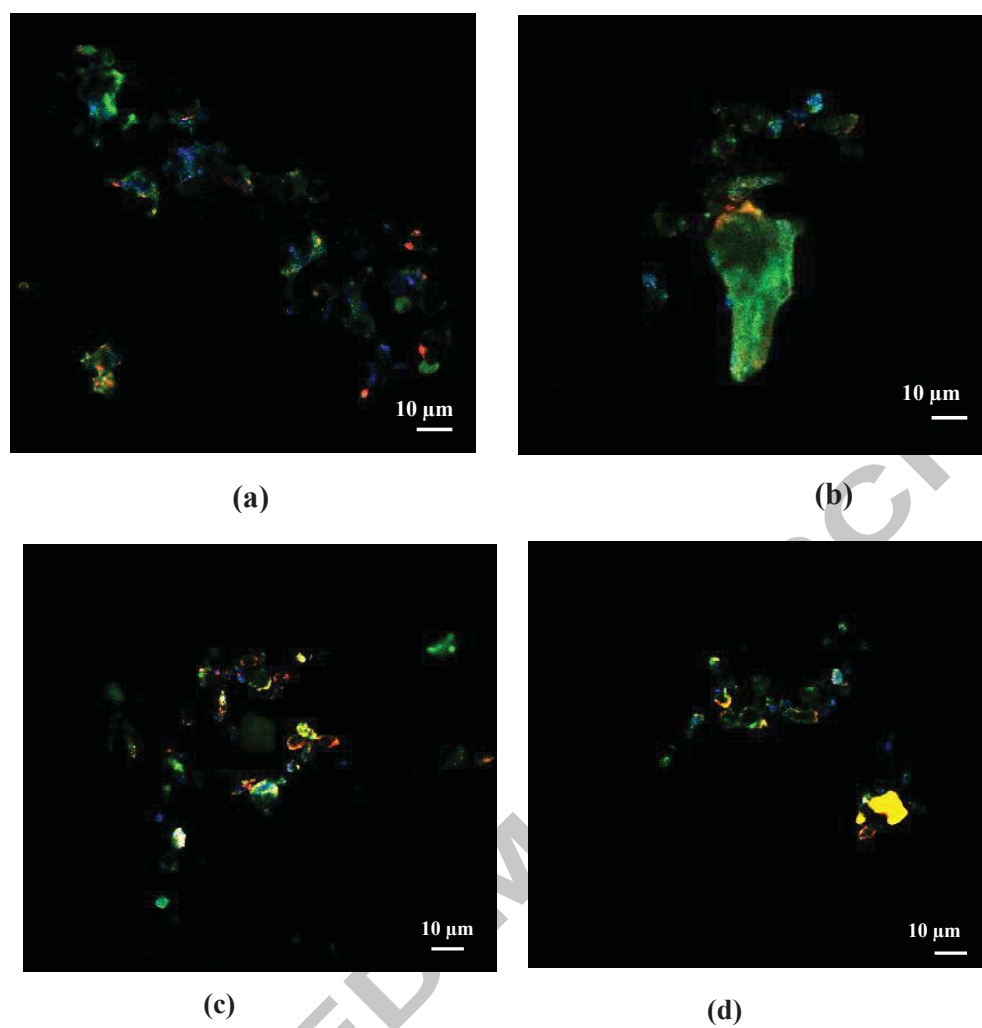


Fig. 5.

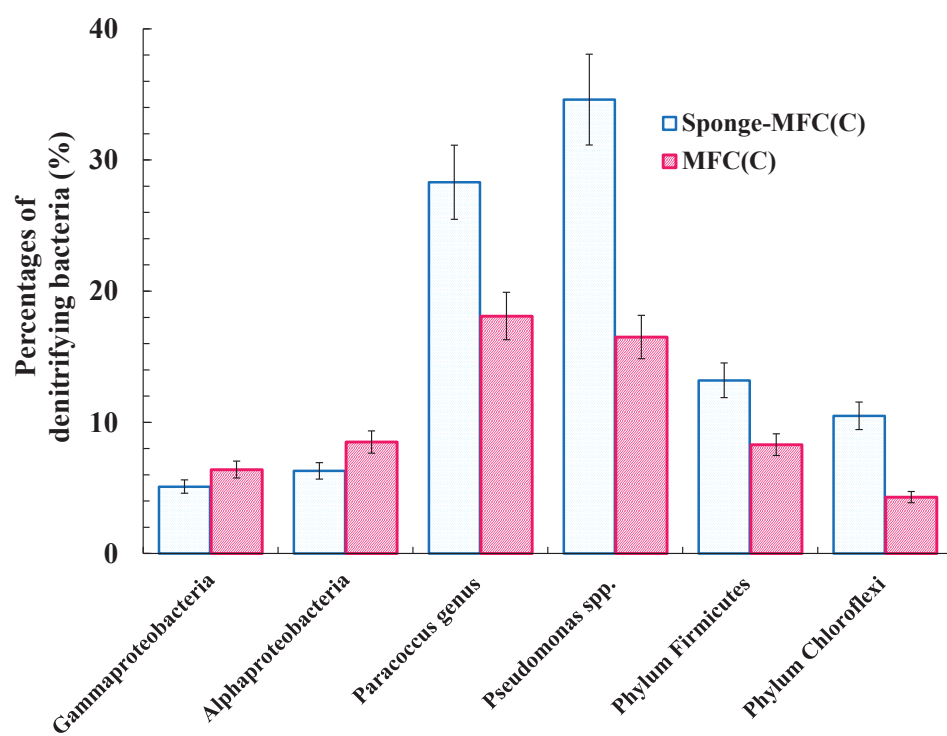


Fig. 6.

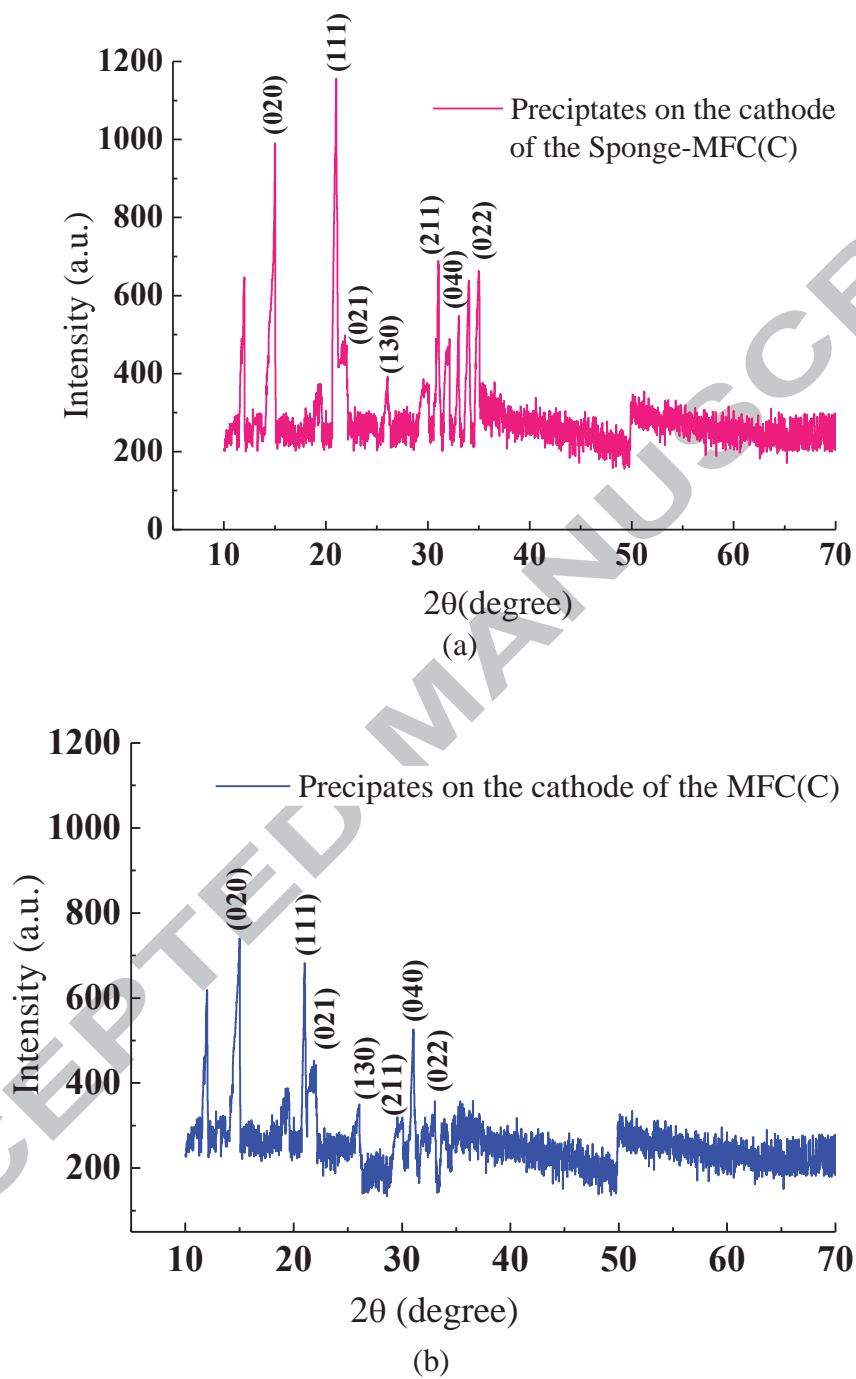
**Fig. 7.**

Table titles

Table 1. Concentrations of $\text{NH}_4\text{-N}$, $\text{NO}_3\text{-N}$, $\text{NO}_2\text{-N}$ and T-N from the effluent of the Sponge-MFC and the MFC under the closed-circuit and open-circuit conditions

Table 2. Distribution of nitrifying and denitrifying bacteria of the sponge in the Sponge-MFC(C) and the Sponge-MFC(O)

ACCEPTED MANUSCRIPT

Table 1.

Concentrations of $\text{NH}_4\text{-N}$, $\text{NO}_3\text{-N}$, $\text{NO}_2\text{-N}$ and T-N from the effluent of the Sponge-MFC and the MFC under the closed-circuit and open-circuit conditions

Reactors	$\text{NH}_4\text{-N}$ (mg/L)	$\text{NO}_3\text{-N}$ (mg/L)	$\text{NO}_2\text{-N}$ (mg/L)	T-N (mg/L)
Sponge-MFC (C)	2.85 ± 0.41	0.12 ± 0.03	0.02 ± 0.01	2.99 ± 0.56
Sponge-MFC (O)	8.63 ± 0.29	10.35 ± 1.43	2.27 ± 0.17	21.25 ± 1.96
MFC (C)	14.36 ± 1.31	3.05 ± 0.15	0.02 ± 0.01	17.43 ± 2.47
MFC (O)	18.09 ± 1.56	16.36 ± 2.54	4.86 ± 1.03	39.31 ± 2.69

Table 2.

Distribution of nitrifying and denitrifying bacteria of the sponge in the Sponge-MFC(C) and the Sponge-MFC(O)

	Bacteria	Sponge-MFC(C)	Sponge-MFC(O)
Denitrifying bacteria at the inner layer of sponge	Gammaproteobacteria	$18.3 \pm 1.6\%$	$44.5 \pm 2.1\%$
	Alphaproteobacteria	$38.4 \pm 2.3\%$	$32.3 \pm 1.9\%$
	Paracoccus genus	$21.2 \pm 2.0\%$	
	Pseudomonas spp.	$10.6 \pm 1.4\%$	
Nitrifying bacteria at the outer layer of sponge	AOB ^a	$23.5 \pm 2.3\%$	$20.3 \pm 2.2\%$
	NOB ^b	$42.5 \pm 3.2\%$	$35.4 \pm 2.9\%$

^a AOB, Ammonium oxidizing bacteria

^b NOB, Nitrite oxidizing bacteria